Distribution of *ABL* and *BCR* Genes in Cell Nuclei of Normal and Irradiated Lymphocytes

By S. Kozubek, E. Lukášová, L. Rýznar, M. Kozubek, A. Lišková, R.D. Govorun, E.A. Krasavin, and G. Horneck

Using dual-color fluorescence in situ hybridization (FISH) combined with two-dimensional (2D) image analysis, the locations of *ABL* and *BCR* genes in cell nuclei were studied. The center of nucleus-to-gene and mutual distances of *ABL* and *BCR* genes in interphase nuclei of nonstimulated and stimulated lymphocytes as well as in lymphocytes stimulated after irradiation were determined. We found that, after stimulation, the *ABL* and *BCR* genes move towards the membrane, their mutual distances increase, and the shortest distance between heterologous *ABL* and *BCR* genes increases. The distribution of the shortest distances between *ABL* and *BCR* genes in the G_0 phase of lymphocytes corresponds to the theoretical distribution calculated by the Monte-Carlo simulation. Interestingly, the shortest *ABL-BCR* distances in G_1 and $S(G_2)$ nuclei are greater in experiment as compared with theory. This result suggests the existence of a certain regularity in the gene arrangement in the G_1 and $S(G_2)$ nuclei that keeps *ABL* and *BCR* genes at longer than random distances. On the other hand, in about 2% to 8% of lymphocytes, the *ABL* and *BCR* genes are very close to each other (the distance is less than ~0.2 to 0.3 μm). For comparison, we studied another pair of genes, *c-MYC* and *IgH,* that are critical for the induction of t(8;14) translocation that occurs in the Burkitt's lymphoma. We found that in about 8% of lymphocytes, *c-MYC* and *IgH* are very close to each other. Similar results were obtained for human fibroblasts. γ-Radiation leads to substantial changes in the chromatin structure of stimulated lymphocytes: *ABL* and *BCR* genes are shifted to the nuclear center, and mutual *ABL-BCR* distances become much shorter in the G_1 and $S(G_2)$ nuclei. Therefore, we hypothesize that the changes of chromatin structure in the irradiated lymphocytes might increase the probability of a translocation during G_1 and $S(G_2)$ stages of the cell cycle. The fact that the genes involved in the t(8;14) translocation are also located close together in a certain fraction of cells substantiates the hypothesis that physical distance plays an important role in the processes leading to the translocations that are responsible for oncogenic transformation of cells.

CHROMOSOMAL abnormalities, including translocations, inversions, insertions, deletions, and numerical aberrations, are frequently detected in human cancer and particularly in leukemias.[1,2] Many of these changes are not random: they have been found specific to a particular subtype of leukemia and often represent the only visible chromosomal alteration in the leukemic cells.[2,3] The phenomenon of cytogenetic-clinicopathologic correlation implies that the genetic event resulting from a specific chromosomal rearrangement must be very important for the pathogenesis of leukemia.[2-4]

Translocations or exchanges of genetic material between chromosomes represent the best characterized cytogenetic abnormalities. The prototype of a translocation associated with leukemia is the t(9;22)(q34;q11) that results in an abnormal chromosome 22 called the Philadelphia chromosome (Ph).[4] This translocation involves an aberrant transfer of the *c-abl* protooncogene from chromosome 9 to the site adjoining the breakpoint cluster region (*bcr*) of the *BCR* gene on chromosome 22.[2] The chimeric *BCR-ABL* gene created by the interchromosomal exchange produces a hybrid mRNA that translates the fusion protein.[5,6] This phenomenon is fundamental in the pathogenesis of chronic myeloid leukemia (CML) and also in a subset of acute lymphoblastic leukemias and acute myelogenous leukemias.[7-9] This chimeric gene is responsible for indolent clonal expansion, with an invariable progression to an aggressive phenotype terminated by blast crisis.[7,10] The breakpoints of *ABL* and *BCR* genes vary widely in location; however, they always occur within introns, resulting in the fusion of specific *ABL* exons in the processed *BCR-ABL* mRNA. Breakpoints of the *ABL* gene occur in a large (200-kb) region in the 5′ portion of the gene, usually in the intron 1, whereas breakpoints in the *BCR* gene occur either between exons 2 and 3 (or 3 and 4; M*bcr*) or between exons 1 and 2 (m*bcr*). Thus, two types of M*abl-bcr* transcripts can be observed that join *BCR* exons 2 or 3 with *ABL* exons 2 through 11. This translocation is observed only in CML. The m*bcr* translocations result in fusion of the first exon of the *BCR* gene with *ABL* exons 2 through 11.[2,10]

Direct studies of atomic bomb survivors and patients treated by x-rays provide strong evidence that ionizing radiation induces both chronic myeloid leukemia and acute types of leukemia.[11] The time trends are as follows: the death rate is already increasing at 2 years after the first exposure, peaking at 3 to 5 years, and declining to the control level more than 20 years after the exposure. From these facts, it seems that radiation induces the formation of *BCR-ABL* chimeric genes. However, the low frequency of such events makes the finding of direct evidence very difficult.[12]

The mechanism of *ABL-BCR* translocation is not known. It is possible that the distance between breakpoint regions in the replicating interphase nucleus influences the exchange of genetic material between the terminal q parts of chromosomes 9 and 22.

Only limited information about the arrangement of chro-

From the Institute of Biophysics, Academy of Sciences, Brno, Czech Republic; the Faculty of Informatics, Masaryk University, Brno, Czech Republic; the Joint Institute for Nuclear Physics, Moscow Region, Russia; and the Deutsche Forschungsanstalt für Luft- und Raumfahrtmedizin, Institut für Luft-und Raumfahrtmedizin, Köln, Germany.

Submitted February 12, 1996; accepted February 10, 1997.

Supported by the Grant Agency of the Czech Republic (Grant No. 202/96/1718) and by the Grant Agency of the Ministry of Health of the Czech Republic (Grant No. 2636-2).

Address reprint requests to Dr Stanislav Kozubek, Institute of Biophysics, Academy of Sciences, Královopolská 135, 612 65 Brno, Czech Republic.

The publication costs of this article were defrayed in part by page charge payment. This article must therefore be hereby marked ''advertisement'' *in accordance with 18 U.S.C. section 1734 solely to indicate this fact.*

0006-4971/97/8912-0033$3.00/0

mosomes and individual genes in the interphase nucleus exists. The nuclear architecture of the eukaryotic genome might be mediated by chromatin attachments to the nuclear matrix and nuclear membrane[13,14] and by higher-order chromatin structures.[15] Individual chromosomes have been shown to occupy distinct territories within mammalian nuclei.[16-18] The results of optical space sectioning of polytene chromosomes of Drosophila larvae show that two apparently identical cells often have different chromosomes as nearest neighbors.[19] Application of the fluorescence in situ hybridization (FISH) technique combined with improved optical microscopy and image processing systems have made it possible to visualize selected chromosomal domains in the interphase nuclei. Results obtained with probes of the constitutive heterochromatin of centromeric regions show their nonrandom distribution.[20-22] Changes in the heterochromatin position of living neurons[23] and a cell-cycle dependent clustering of human centromeres in the G_1 phase that are dispersed as cells move into the S phase (observed by Bartholdi[24]) provide evidence that the centromeric heterochromatin might be specifically localized in certain cell types, whereas it is randomly distributed in others. Höfers et al[25] suggest that these conclusions on localization of centromeric heterochromatin could be valid for any chromosome locus.

To obtain information about localization of *abl* and *bcr* regions in the interphase nuclei of human lymphocytes, we analyzed images of cell nuclei obtained semiautomatically with a high-resolution CCD camera using software that characterizes the positions of two FISH signals of different colors. We used an M*bcr* probe modified with digoxigenin and an *abl* probe modified with biotin. The following measurements were taken: (1) the distances from the center of nucleus to genes *ABL* and *BCR*; (2) the distance between the two homologous green-stained *ABL* genes; (3) the distance between the two homologous red-stained *BCR* genes; and (4) the distance between the *ABL* and *BCR* genes.

Because of the high frequency of leukemias in individuals exposed to ionizing radiation, we performed similar measurements in lymphocytes irradiated before stimulation with 5 Gy of γ-rays to detect possible changes in the localization of *ABL* and *BCR* genes induced by the radiation.

To further support the hypothesis that a short distance between genes participating in translocation increases the probability of such an event, we investigated the distances between *c-MYC* and *IgH* loci in human lymphocytes and fibroblasts. The telomere 14q probe used in our experiments hybridizes to specific sequences at 14q32.3 that are located near the heavy-chain locus of immunoglobulin (*IgH*).[26,27] Translocations that involve the *IgH* locus are very frequent in many B-cell tumors; this genetic lesion results in the deregulation of an oncogene as a consequence of the translocation. Activation of the *c-MYC* oncogene is a central event in Burkitt's lymphoma. A characteristic chromosomal translocation t(8;14)(q24;q32), seen in 75% to 85% of patients, puts the *c-MYC* oncogene close to an *IgH* locus. Presumably, this rearrangement arises by random malfunctioning of the recombinase during maturation of B cells.[27-29] Exchange of DNA between the two chromosomal positions implies that they are physically close to each other at the time this event occurs.[30] Therefore, the occurence of a fraction of cells with *c-MYC* and *IgH* loci in close vicinity will substantiate the hypothesis that physical distance plays an important role in the processes leading to translocations responsible for oncogenic transformation.

MATERIALS AND METHODS

Cultivation and Irradiation of Lymphocytes

The lymphocytes were isolated from the whole heparinized blood (16 to 20 U/mL) of healthy individuals. Plasma containing lymphocytes was obtained after 2 hours of blood sedimentation at room temperature. It was divided into two 3-mL aliquots and irradiated by 0 and 5 Gy of ^{137}Cs γ-rays (0.66 MeV; dose rate 3.6 Gy/min), respectively. Control and irradiated samples were diluted (1:3) with RPMI-1640 medium containing 0.1 mL of phytohaemagglutinin (PHA; Murex, Dartford, UK) per 5 mL of the suspension, 1% glucose, penicillin (100 U/mL), and streptomycin (100 μg/mL). The incubation was performed at 37°C for 50 hours. Colcemid was added 2 hours before the end of incubation. After hypotonic treatment (0.075 mol/L KCl), the nuclei were fixed in methanol/acetic acid (3:1) and the suspension was dropped on slides and allowed to dry.

Cell Cycle Analysis Using a Microscopic Method

The cell nuclei were classified as G_0, G_1, and S(G_2) using a microscopic method.[31] Two main characteristics were determined microscopically: the radius of cell nucleus and the number of doublets, ie, signals on both chromatids after DNA duplication. Small nuclei (radius <5 μm) were considered as nonstimulated in the G_0 phase of the cell cycle.[31] Large nuclei with only one signal of each of the *ABL* and *BCR* genes were grouped in the G_1 phase; the nuclei with a double signal for at least one of these genes were grouped in the S(G_2) phase. Nonstimulated lymphocytes were distinguished from other white blood cells by their large and round nucleus. Results were compared with flow cytometric data (G_0+G_1, S, and G_2) obtained at different periods after stimulation of both control and irradiated lymphocytes. Another criterion used was the number of centromeres[31] that were visualized using a pancentromeric DNA probe.

Flow Cytometric Analysis

Lymphocytes were fixed in three successive baths of methanol/acetic acid mix (3:1) at −20°C for 15 minutes each. After washing in phosphate-buffered saline, the cells were resuspended in a buffer containing 50 μg/mL propidium iodide, 10 mmol/L Tris-HCl, pH 7.5, 5 mmol/L $MgCl_2$, and 10 μg/mL RNase A. Finally, the cells were analyzed on a Coulter Epics XL flow cytometer (Coulter, Hialeah, FL). In most cases, 2×10^4 cells were recorded per sample. DNA distribution was calculated using standard software.

DNA Probes, In Situ Hybridization, and Probe Detection

M*bcr-abl* (digoxigenated *bcr*, biotinylated *abl*), digoxigenated *c-myc*, and biotinylated unique telomere 14q DNA probes were purchased from Oncor (Gaithersburg, MD), hybridized, and detected according to earlier published recommendations,[32] with small modifications. The chromosomes were denatured at 70°C in 70% formamide with 2× SSC, pH 7, for 2 minutes; dehydrated in cold (−20°C) 70%, 80%, and 95% ethanol (2 minutes each); and then air dried.

The probe was prewarmed at 37°C for 5 minutes and vortexed. The M*bcr-ab*l DNA probe (10 μL) or a mixture of 10 μL telomere 14 and 7 μL of *c-myc* probes was applied to the denatured and dry slide, covered by a glass coverslip of 25 × 25 mm, sealed with

rubber cement, and incubated overnight at 37°C in a humidified chamber in a perfect horizontal position.

Posthybridization washing was performed in 50% formamide with 2× SSC, pH 7, at 43°C for 15 minutes, followed by two 5-minute washes in 2× SSC containing 0.1% Tween 20, pH 7, at 37°C. Slides were then transferred to 1× PBD (Oncor) and incubated at room temperature for 3 minutes. Rhodamine-antidigoxigenin and fluorescein isothiocyanate (FITC)-avidin (60 μL) was applied to a slide and incubated for detection under a plastic coverslip at 37°C for 5 minutes. The washing was performed in three changes of 4× SSC containing 0.1% Tween 20, pH 7, at 43°C for 5 minutes. The temperature of the slides was equilibrated to room temperature in the 4× SSC containing 0.1% Tween 20, and the cells were contrastained with 4′,6-diamidine-2′-phenylindole (DAPI; 0.02 μg/mL) in the Vectashield (Vector, Burlingame, CA).

Data Acquisition and Statistical Analysis

The green and red fluorescent signals for *abl* and *bcr* genes were detected on a blue background. Digital images were generated using a single-chip cooled color camera (Hamamatsu C5310; Hamamatsu Photonics K.K., Shimokanzo, Japan). The camera was attached to a Jenalumar epifluorescence microscope (Carl Zeiss GmbH, Jena, Germany) equipped with dual-band and triple-band filters (AHF, Tübingen, Germany) for FITC-PI and FITC-PI-DAPI, respectively. The images were digitized (MuTech Image/VGA Plus frame-grabber; MuTech Corp, Woburn, MA) with 24-bit resolution (8 bits per color) and processed using a Pentium 100 MHz computer (AutoCont s.r.o., Brno, Czech Republic).

A special software, FISH 1.1 (M. Kozubek, Institute of Biophysics, Academy of Sciences, Brno, Czech Republic), was developed for the automated analysis of the FISH-painted nuclei.[33] FISH 1.1 runs under the MS-Windows environment and contains a number of filters and procedures for image analysis.

The nuclei were detected using simple thresholding in blue color. The optimal threshold was found by an automatic histogram analysis. The green and red signals inside nuclei were detected by means of a modified watershed algorithm.[33,34]

To detect exactly two green (red) signals for *ABL* (*BCR*) genes, the following steps were applied. (1) The nucleus was excluded from the final data set if no or just one green (red) signal was found. (2) The nucleus was excluded if the intensity of the third highest (green or red) signal found on the nucleus was stronger than two thirds of the intensity of the second highest signal. (3) The nucleus was accepted otherwise, taking into account only the two highest signals.

The coordinates of the signals, the distance of the signals from the center of the nucleus (in percentage of local radius), their intensity, and their area were computed. To confirm the results of the analysis, the signals were visualized on a screen. After the analysis of each image, text files were generated with information about the image, each nucleus on the image, and each signal on a given nucleus. An appropriate format of the text file was chosen for the import of the whole data set into SigmaPlot (Jandel Scientific, San Rafael, CA). Two-dimensional (2D) projections of the distances between the signals and additional characteristics were calculated using the Transform option of SigmaPlot. All distances between fluorescent signals in the interphase nuclei of lymphocytes were determined as projections. The significance of the differences between various distributions was calculated using the Student's *t*-test option of SigmaPlot at $P = .05$.

The lymphocytes increased in diameter after stimulation [from ~10 μm in the G_0 phase up to 16 μm in the S(G_2) phase]. Therefore, all distances are expressed as the percentage of nuclear radius.

Calculation of Theoretical Distributions

The following notation will be used throughout the remainder of this paper: (1) AA, distances between homologous *ABL-ABL* genes; (2) BB, distances between homologous *BCR-BCR* genes; (3) AB_m, minimum of four distances *ABL-BCR* in nucleus; (4) CA, distances between nuclear weight center and *ABL* gene in terms of percentage of local radius (local radius is the distance between the nuclear center and the membrane in the direction of the *ABL* [*BCR*] gene); (5) CB, distances between nuclear weight center and *BCR* gene. The average values of the above-mentioned distances will be $\overline{\mathbf{AA}}$, $\overline{\mathbf{BB}}$, $\overline{\mathbf{CA}}$, $\overline{\mathbf{CB}}$, and $\overline{\mathbf{AB_m}}$. In the case of dual-color probes for telomere 14q and *c-MYC,* the same notation will be used with the letters T and M, ie, TT, MM, TM_m, CT, and CM.

It will be shown later that in all phases of the cell cycle of lymphocytes the distribution of CA and CB distances does not correspond to random location of the *ABL* and *BCR* genes in a sphere. The average distance of a point, randomly placed in a sphere, from the center of the sphere in the 2D projection is 58.8% of radius, which is much more than $\overline{\mathbf{CA}}$ and $\overline{\mathbf{CB}}$ (see the Results). It means that the genes are situated preferentially at certain distances from the center. Reconstruction of the three-dimensional distribution of CA or CB distances is possible under the condition that the nuclei are rotationally symmetrical, ie, that the distribution of genes in spherical concentric layers is random (although the genes can be situated preferentially at certain layers). This approach will be called

Table 1. Distribution of Lymphocytes in Different Phases of the Cell Cycle as a Function of the Time of Stimulation Determined From Flow Cytometric and Microscopic Data

Radiation Dose (Gy)	Time of Stimulation (h)	No. of Cells (%)			
		G_0	G_1	S	G_2
0	0	83.0 ± 5.4	14.0 ± 2.9	3.0 ± 2.9	0 ± 2.5
	20	56.0 ± 6.3	28.2 ± 2.8	14.5 ± 3.8	1.3 ± 2.5
	30	17.0 ± 6.9	65.1 ± 4.4	13.2 ± 4.1	4.7 ± 2.8
	40	78.7 ± 6.3*		15.8 ± 3.6	5.5 ± 2.7
	50	25.0 ± 2.6	54.7 ± 4.2	10.6 ± 3.7	9.7 ± 3.1
5	20	80.9 ± 6.2*		12.5 ± 3.4	6.5 ± 2.8
	30	30.0 ± 2.7	43.4 ± 3.0	17.6 ± 3.1	8.0 ± 2.6
	40	76.2 ± 6.9*		13.7 ± 3.8	10.1 ± 3.1
	50	26.0 ± 2.5	51.7 ± 5.0	12.0 ± 4.1	10.3 ± 3.4

The cell cycle phases were determined by flow cytometry ($G_0 + G_1$, S, and G_2) and according to the nuclear radius (R)[31] ($R < 5$ μm for G_0, $R > 5$ μm for $G_1 + S + G_2$).

* Microscopic analysis was not performed.

the model of rotational symmetry (RS model). Calculation of the distributions in the RS model is quite simple. Four points (simulating *ABL* and *BCR* genes) are placed in a sphere using weighted random number generator with different weights at different layers. For each quadruple of points, the values of AA, BB, AB_m, CA, and CB are calculated. The procedure is repeated about 10^5 times, and distributions of all distances are generated. The probabilities of gene appearance in different layers (weights of random number generator) are adjusted in such a way that the theoretical distributions of CA and CB distances in projection reproduce the experimental histograms.

Using the RS model, the distributions of AA, BB, and AB_m distances based on experimental CA and CB histograms were calculated and compared with the experimental AA, BB, and AB_m histograms.

RESULTS

The center-to-gene distances as well as the distances between genes in nuclei were measured in the intact and irradiated lymphocytes both immediately after the addition of PHA and after 50 hours of incubation. All experiments were repeated three times; for each iteration, 200 cell nuclei were analyzed.

After 50 hours of incubation, the lymphocytes are mostly stimulated. The proportion of cells in the G_0, G_1, and $S(G_2)$ stages was approximately 30%, 40% to 50%, and 20% to 30%, respectively, in both the control and irradiated samples. Flow cytometric and microscopic data that express the distribution of lymphocytes in the different stages of the cell cycle as a function of the time of stimulation are shown in Table 1.

Center-to-Gene Distributions of ABL and BCR Genes (CA and CB Distributions)

Nonirradiated controls. The center-to-gene distributions of the *ABL* and *BCR* genes (CA and CB distributions) are shown in Fig 1 A and B. The mean values of these distances ($\overline{\mathbf{CA}}$ and $\overline{\mathbf{CB}}$) are significantly lower for cells in the G_0 phase compared with cells in the G_1 and $S(G_2)$ phases (Table 2). The shape of the distributions of nuclear center-to-gene distances changes from narrow for cells in the G_0 phase to broad in the G_1 phase and again to narrow one in the $S(G_2)$ phase (Fig 1A, B, and E). The distances CB are significantly longer than the distances CA for cells in the G_0 phase; they are equal in the G_1 phase and shorter in the $S(G_2)$ phase (Table 2). Thus, for cells in the G_0 phase, chromosome 22 is more distant from the nuclear center than chromosome 9, whereas chromosome 22 is closer to the nuclear center for cells in the $S(G_2)$ phase.

After γ-irradiation. The *ABL* and *BCR* genes are located closer to the nuclear center in both the G_1 and $S(G_2)$ lymphocytes irradiated with 5Gy of γ-rays (Fig 1C and D). Compared with control samples, the distributions have smaller distances. Changes in the $S(G_2)$ phase are more pronounced compared with cells in the G_1 phase. The difference between the center-to-gene average distances of *ABL* and *BCR* genes ($\overline{\mathbf{CA}}$ and $\overline{\mathbf{CB}}$) is not statistically significant for cells in the G_1 phase; at the same time, for cells in the $S(G_2)$ phase, the center-to-gene distances for *BCR* genes are shorter than for *ABL* genes ($\overline{\mathbf{CB}}<\overline{\mathbf{CA}}$). The results clearly show that, after

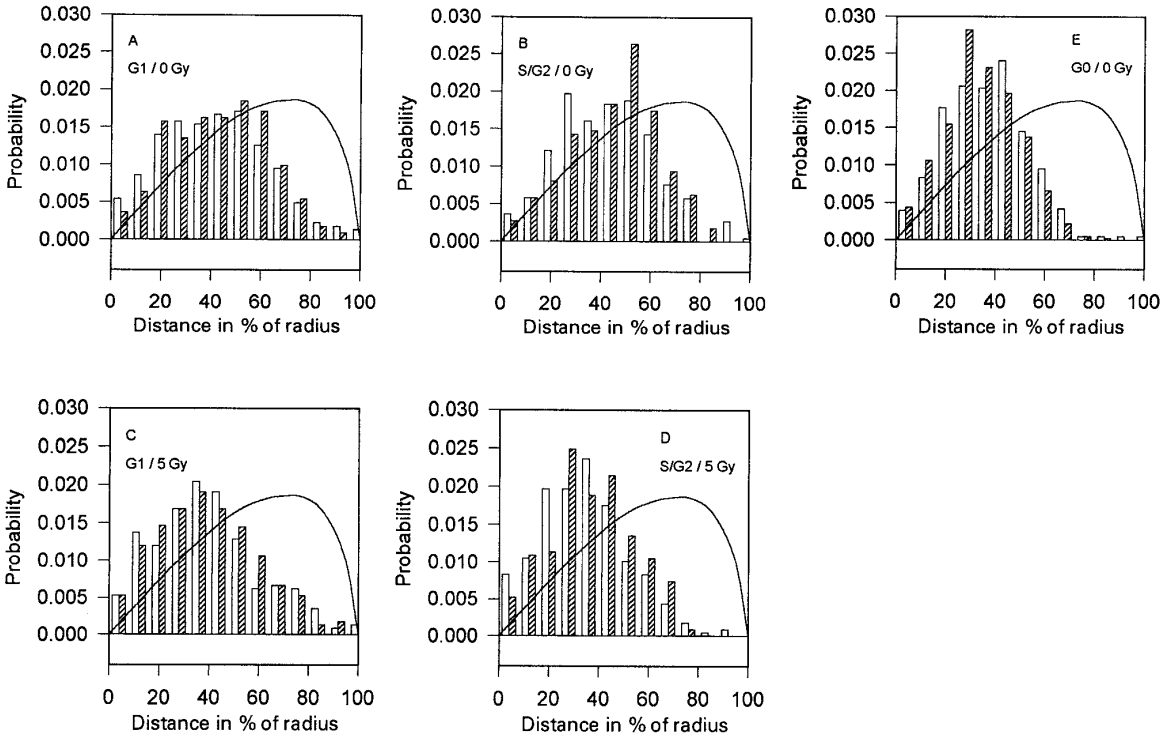

Fig 1. Distances between the nuclear center and *BCR* (*ABL*) genes (CB and CA). Distribution of the 2D projections of the distances between the *BCR* (□) or *ABL* (▨) genes and the center of nucleus (CB and CA) of the control (A, B, and E) and the γ-irradiated (5 Gy; C and D) human lymphocytes. The mean values and standard deviations are given in Table 2. The corresponding theoretical distributions of the 2D projections of the distances between the center of the sphere and the point randomly placed inside the sphere are shown by the solid line.

Table 2. The Average Values and Standard Deviations of the AA, BB, AB_m, CA, and CB Distributions in Interphase Nuclei of Control and Irradiated Lymphocytes

Phase of Cell Cycle	Irradiation (Gy)	$\overline{AA}$ (% of R)	$\overline{BB}$ (% of R)	$\overline{AB}_m$ (% of R)*	$\overline{CA}$ (% of R)	$\overline{CB}$ (% of R)
G_0	0	57.3 ± 1.5 (55.8)†	53.4 ± 1.3 (52.2)	24.0 ± 0.9 (25.4)	34.9 ± 0.7	37.4 ± 0.7
G_1	0	63.0 ± 1.8 (59.3)	57.9 ± 1.7 (55.2)	34.5 ± 1.1 (30.2)‡	43.5 ± 0.8	42.9 ± 0.9
$S(G_2)$	0	61.9 ± 1.8 (60.9)	59.4 ± 1.5 (58.7)	36.0 ± 1.0 (31.7)‡	45.6 ± 0.7	43.3 ± 0.7
G_1	5	60.2 ± 1.4 (54.2)	59.8 ± 1.7 (55.5)	26.6 ± 1.0 (28.6)	39.6 ± 0.8	40.0 ± 0.9
$S(G_2)$	5	52.1 ± 1.2 (50.9)	49.7 ± 1.4 (47.1)	28.4 ± 0.9 (27.4)	37.3 ± 0.7	35.1 ± 0.7
G_1 (5 Gy/0 Gy)		0.957 ± 0.049	1.033 ± 0.058	0.772 ± 0.052§	0.911 ± 0.035‖	0.933 ± 0.038‖
$S(G_2)$ (5 Gy/0 Gy)		0.842 ± 0.044§	0.837 ± 0.044§	0.789 ± 0.047§	0.818 ± 0.027§	0.811 ± 0.031§
0 Gy (G_1/S)		1.017 ± 0.058	0.975 ± 0.052	0.957 ± 0.056	0.954 ± 0.031	0.990 ± 0.037
5 Gy (G_1/S)		1.156 ± 0.053§	1.204 ± 0.067‖	0.936 ± 0.066	1.062 ± 0.040	1.139 ± 0.048

The distances are shown as a percentage of the nuclear radius (R).

Abbreviations: $\overline{AA}$, average distance *ABL-ABL;* $\overline{BB}$, average distance *BCR-BCR;* $\overline{AB}_m$, average minimum distance *ABL-BCR;* $\overline{CA}$, average distance center of nucleus-to-*ABL;* $\overline{CB}$, average distance center of nucleus-to-*BCR.*

* Minimum of 4 distances between 2D projections of *ABL* and *BCR* genes in a nucleus is taken.

† Theoretical values (in parentheses); the standard errors of the theoretical values (derived from the standard errors of the average center-to-gene distances) are less than that of experimental ones.

‡ Theoretical value is significantly different from the experimental one ($P < .05$).

§ Significantly different from 1 ($P < .005$).

‖ Significantly different from 1 ($P < .05$).

irradiation, *ABL* and *BCR* genes are situated in close proximity to the nuclear center compared with the nonirradiated control.

Comparison of theoretical, random distributions of genes in a sphere with our experimental data strongly suggests that the location of both *ABL* and *BCR* genes is not random for all stimulated, nonstimulated, irradiated, and nonirradiated lymphocytes (Fig 1A through E).

Distance Between Homologous ABL and BCR Genes (AA and BB Distances)

Nonirradiated controls. The distances between the homologous *abl* and *bcr* regions were determined for both irradiated and nonirradiated lymphocytes in the G_0, G_1, and $S(G_2)$ phases of the cell cycle (Fig 2A through E). The average distance between *ABL(BCR)* genes on homologous chromosomes in the G_0 phase is significantly shorter than the same distance in the G_1 or $S(G_2)$ phases (Table 2). Generally, in all of these cells, homologous *BCR* genes are closer together than homologous *ABL* genes (**$\overline{BB}$<$\overline{AA}$**). The differences in the distances of these genes in the G_1 and $S(G_2)$ cell nuclei are not significant. Theoretical distributions of distances between homologous *ABL* and *BCR* genes calculated according to the RS model correspond quite well to the experimental ones (Fig 2A, B, and E); the only exceptions are distances between 30% to 50% of the nuclear radius that are more frequent than the theoretical distances.

After γ-irradiation. In irradiated nuclei, the distances between homologous *ABL* as well as *BCR* genes in the $S(G_2)$ stage of the cell cycle are substantially shorter than in nonirradiated nuclei ($P < .05$ for *BCR* and $P < .02$ for *ABL* regions; Fig 2C and D). These distances are not significantly different between irradiated and nonirradiated cells in the G_1 phase (Table 2); however, in the irradiated nuclei, *BCR* genes are closer to each other.

Distance Between ABL and BCR Genes (AB_m Distances)

Nonirradiated controls. The distances between each *ABL* gene (green) to one or another *BCR* gene (red) were determined. The minimum value of the four measured distances per cell nucleus was determined (AB_m). The distances AB_m for each stage of the cell cycle are plotted as normed histograms in Fig 3A, B, and E. The distributions generated by Monte-Carlo calculations according to the RS model are shown by curves in Fig 3A, B, and E. In both G_1 and $S(G_2)$ cell nuclei, the theoretical AB_m distances between nonhomologous genes are significantly shorter ($P < .05$) than experimental AB_m distances (Fig 3A and B and Table 2). No significant difference in the experimental distributions of AB_m distances between cells in the G_1 and $S(G_2)$ phases of the cell cycle exists. In the G_0 phase, the detected distances between nonhomologous genes (Fig 3E) correspond to the theoretical prediction (solid line in Fig 3E and Table 2).

After γ-irradiation. In lymphocytes irradiated with 5 Gy of γ-rays, the average minimum distance between *ABL* and *BCR* genes is substantially shorter than in the nonirradiated lymphocytes (Fig 3C and D and Table 2). This distance (AB_m) decreases from 34.5% to 26.6% of the cellular radius for G_1 cells and from 36.0% to 28.4% for the $S(G_2)$ cells (the differences are significant at $P < .01$). The percentage of cells in which one of the green signals (*ABL*) is located in very close proximity to one of the red (*BCR*) signals (≤0.2 to 0.3 μm) increases (Fig 3) from 2.0% ± 1.0% to 4.1% ± 1.8% in the G_1 phase and from 1.5% ± 1.1% to 5.9% ± 2.2% in the $S(G_2)$ phase. Notably, the percentages for irradiated cells are substantially higher than the theoretically predicted ones (Fig 3C and D, the first column). Differences between irradiated and nonirradiated lymphocytes are not statistically significant. However, an increased number of lymphocytes with *ABL* and *BCR* genes located close together was repeatedly observed after irradiation; the same phenom-

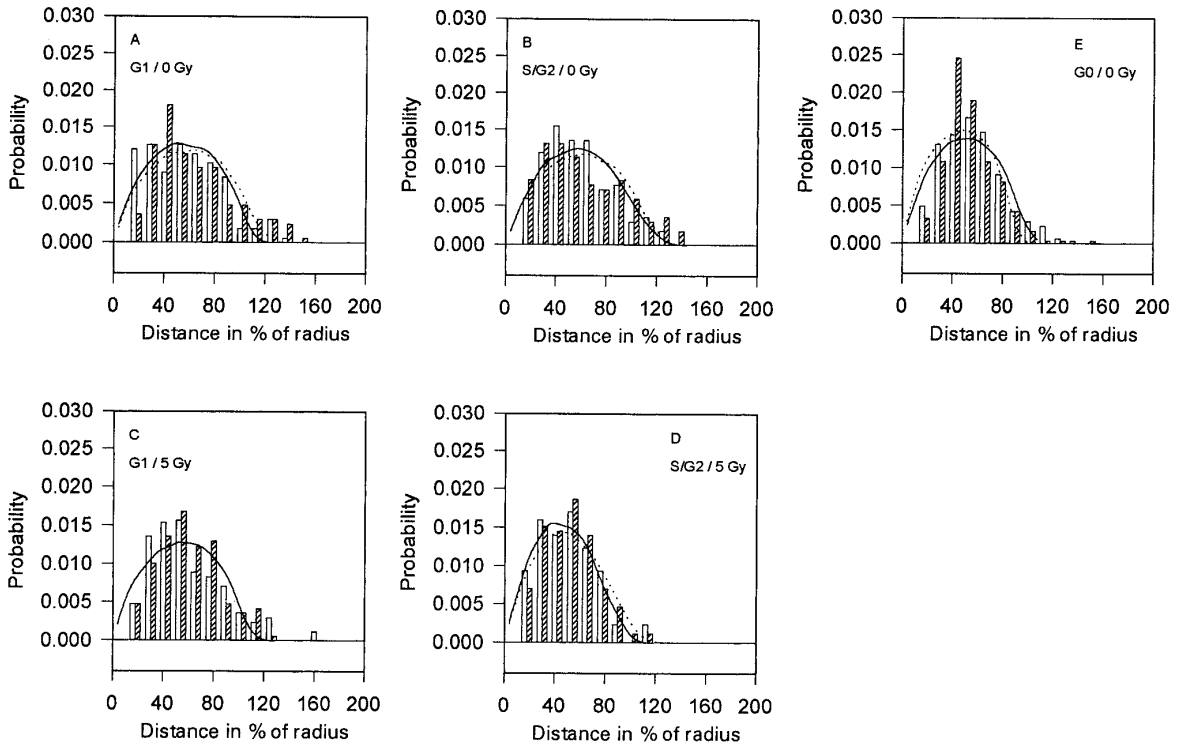

Fig 2. Distances between homologous *BCR* and *ABL* genes (BB and AA). Distributions of 2D-projections of the distances between homologous *BCR* genes (□) and *ABL* genes (▨) in the control (A, B, and E) and in the γ-irradiated (5 Gy; C and D) human lymphocytes. The mean values and standard deviations are given in Table 2. The full (dotted) curves represent the corresponding theoretical distributions calculated by Monte-Carlo simulation using experimentally determined center-to-gene distributions from Fig 1 (according to the RS model).

enon was also observed in the fibroblasts in which the number of such nuclei was higher than predicted theoretically even in the nonirradiated cells (results not shown).

DISCUSSION

Using dual-color FISH combined with 2D image analysis, we measured the 2D projections of center of nucleus-to-gene distances for *ABL* and *BCR* genes and mutual distances between both homologous and heterologous *ABL* and *BCR* genes in interphase lymphocytes. We found that, after the stimulation of lymphocytes, the *ABL* and *BCR* genes move towards the membrane, their mutual distances increase, and the minimum distance between heterologous *ABL* and *BCR* genes increases. The experimental distribution of the shortest distances between *ABL* and *BCR* genes (AB_m distribution) in the G_0 phase of lymphocytes corresponds to the theoretical AB_m distribution calculated according to the RS model (see the Materials and Methods). On the other hand, experimentally measured AB_m distances are greater than AB_m distances determined theoretically (using RS model) for cells in the G_1 and $S(G_2)$ phases, giving evidence of a special type of nonrandom arrangement. The transition of lymphocytes from the G_0 phase to the G_1 and $S(G_2)$ phases involves rearrangement of chromatin manifested by prolongation of minimal distances between *ABL* and *BCR* genes that exceeds the calculated random distances. This nonrandom arrangement of *ABL* and *BCR* genes is also evidenced by the more frequent (as compared with the theoretical calculation) occurrence of cells with two homologous genes at a distance of 30% to 50% of the nuclear radius (Fig 2A and B). Nonrandom spatial distribution of *ABL*, *BCR*, and chimeric *BCR-ABL* genes was also observed in bone marrow cells of CML patients.[35]

Ionizing radiation partially inhibits the changes in *ABL* and *BCR* localization induced in the lymphocytes by stimulation with PHA. This effect is most pronounced during the $S(G_2)$ phase. In these irradiated lymphocytes, *ABL* and *BCR* genes are near the center of nucleus, the distances between both homologous and heterologous genes are shorter, and the minimum distance between heterologous genes is substantially shorter.

Ionizing radiation induces a wide spectrum of molecular lesions in DNA, including single-strand breaks, double-strand breaks, base damage, and DNA-protein cross-links.[36,37] The majority of DNA breaks are repaired within 10 minutes after irradiation.[38] However, the repair process of double-strand breaks involves mistakes that lead to chromosomal aberrations.[36,38-40] Unrepaired or misrepaired double-strand breaks or chromosomal aberrations might be one possible cause of chromatine changes in stimulated lymphocytes. In addition, a loss of supercoiling ability was observed in irradiated cells.[41,42] The investigators hypothesize that the loss of superhelical density could be attributed to the irreparable lesions induced by radiation. It is possible that the

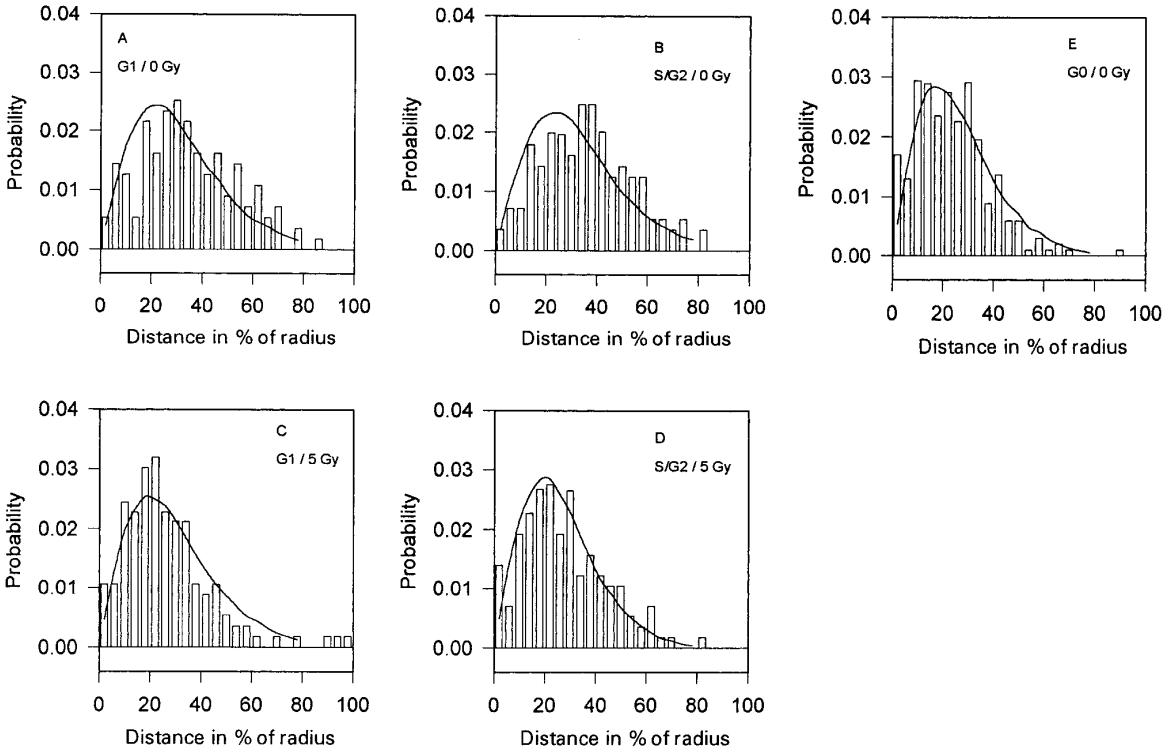

Fig 3. Minimum distances between nonhomologous *BCR* and *ABL* genes (AB_m). Distributions of 2D projections of the minimum distances between the *BCR* and *ABL* genes in the control (A, B, and E) and in the γ-irradiated (5 Gy; C and D) human lymphocytes. The mean values and standard deviations are given in Table 2. The curves represent the theoretical distributions calculated by Monte-Carlo simulation using experimentally determined center-to-gene distributions from Fig 1 (according to the RS model).

chromatine changes in irradiated lymphocytes observed in our experiments could be related to a lower superhelical density of chromatin resulting from irradiation.

The distribution of *ABL-BCR* distances in the irradiated cells corresponds quite well to the RS model. This result means that the nonrandom structural arrangement of *ABL-BCR* genes in the stimulated cells changed after irradiation. In a fraction of irradiated cell nuclei (about 5%), the *ABL* and *BCR* genes are very close to each other ($<$0.2 to 0.3 μm). This fraction is substantially larger than the fraction theoretically predicted from random superposition of signals in the 2D projection. The reason for this stickiness of *ABL* and *BCR* regions is unknown, but one possibility could be an association based on homology of DNA in certain regions of these genes.[30] It is tempting to speculate that physical distance and translocation frequency between specific sequences are correlated. Direct evidence of the induction of *BCR-ABL* fusion by a high dose of X-irradiation in HL60 cells in vitro was reported by Ito.[12]

To further substantiate the hypothesis that physical distance of specific sequences increases the translocation frequency, we investigated the distance distributions of the *c-MYC* gene and unique telomere 14q sequences situated in close proximity of the *IgH* gene. Both of these locuses are involved in the translocation t(8;14) (q24.1;q32.3) in Burkitt's lymphoma. It is supposed that the t(8;14) translocation arises through a malfunction of the recombinases that rearrange the *IgH* gene during maturation of B cells.[27-29] The results of our investigations using lymphocytes and fibroblasts are shown in Fig 4. Distances between heterologous *c-MYC* and telomere 14q sequences are distributed according to the RS model, with the exception of those cases in which the genes are very close to each other ($<$0.2 to 0.3 μm). The number of nuclei with *c-MYC* and telomere 14q sequences that are close to each other is many times higher than the number resulting from theoretical distribution. This difference is significant in both cell types (lymphocytes and fibroblasts), which supports the hypothesis that the association of these genes is related to some mechanism that is cell-type nonspecific. Homology of DNA sequences might serve as a basis of one of such mechanisms.

Exchange of DNA between two chromosomal positions implies that they are physically close together at the time this event occurs.[30] Consequently, the frequency of translocations in cells should increase if the physical distance between critical genes is reduced. We found substantially reduced physical distance between *ABL* and *BCR* genes in irradiated human lymphocytes in the G_1 and $S(G_2)$ stages after stimulation. We also found that the genes involved in the t(8;14) translocation between *c-MYC* and *IgH* loci are frequently close to each other already in the control (nonirradiated) lymphocytes and fibroblasts. The proximity of *c-MYC* to *IgH* loci increases the accessibility of some of their sequences to the recombinase responsible for assemblage of the Ig gene

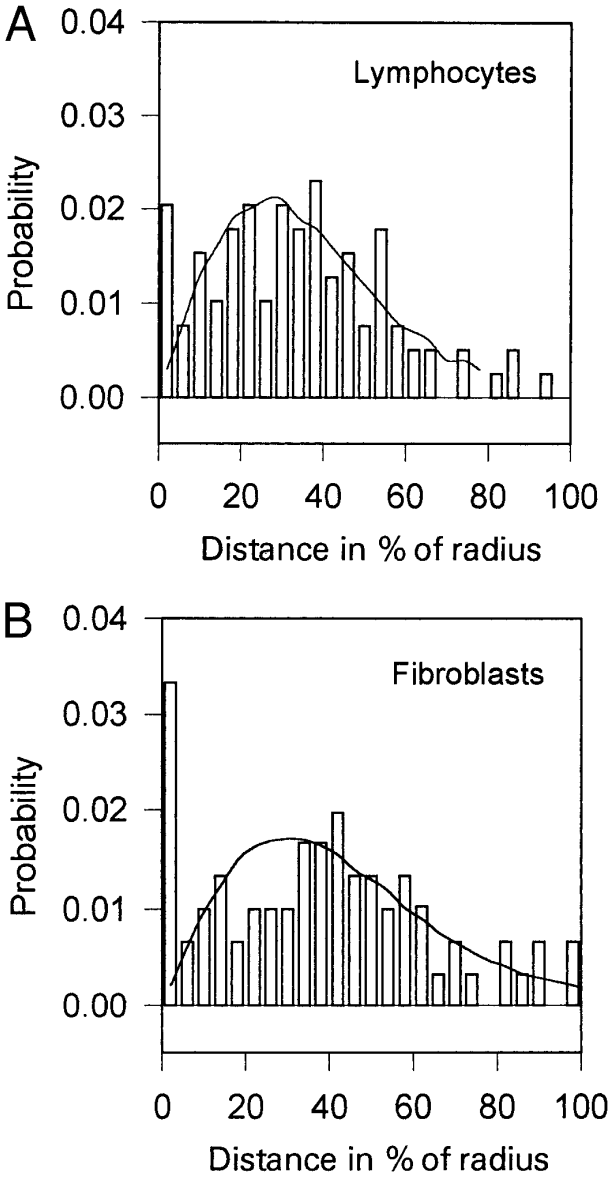

Fig 4. Distributions of the distances between *c-MYC* and unique telomere 14q sequences (TM_m; lying adjacent to the Ig heavy chain locus) in human lymphocytes incubated for 50 hours with PHA (A) and in human fibroblasts (B). The curves represent the theoretical distributions calculated by Monte-Carlo simulation using experimentally determined center-to-gene distributions (not shown). Human fibroblasts (VF-10) were grown in RPMI medium supplemented with 10% fetal calf serum, 0.5% L-glutamine, 1% glucose, and antibiotics at 37°C to the confluent state.

during B-cell development. Through mistakes in this gene rearrangement mechanism, the translocation between *c-MYC* and *IgH* loci can appear in B cells. The translocations are manifested as Burkitt's lymphoma. The mechanism of Ig genes rearrangement is limited only to lymphoid cells; therefore, the physical proximity of *c-MYC* to *IgH* loci in fibroblasts cannot lead to their translocation.

We conclude that the locations of genes in the interphase nucleus are not fully random. Their organization can be characterized by the following principles. (1) The genes can be localized most commonly at a specific range of distances between the nuclear center and membrane (in a spherical layer). This type of nonrandom organization of genes in nuclei makes it possible to describe the structure by the RS model (see the Materials and Methods), which gives in many cases reasonably good results. (2) Two homologous or heterologous genes inside the layer can be located at preferential mutual positions. This principle is manifested by the discrepancy between experimentally observed distributions of gene-to-gene distances and the corresponding theoretical distribution calculated on the basis of RS model. (3) Two heterologous genes can be associated at very short distances (stickiness of genes). For homologous genes, this phenomenon is observed in $S(G_2)$ cells.

These principles are valid for the organization of cell nucleus in dependence on other factors such as the type of the cell, the phase of the cell cycle, the state of the cellular environment, and, of course, the characteristics of the genes themselves.

REFERENCES

1. Rabbitts TH: Chromosomal translocations in human cancer. Nature 372:143, 1994

2. Pui CH, Crist WM, Look AT: Biology and clinical significance of cytogenic abnormalities in childhood acute lymphoblastic leukemia. Blood 76:1449, 1990

3. Melo JV: The molecular biology of chronic myeloid leukaemia. Leukemia 10:751, 1996

4. Kurzrock R, Gutterman JL, Talkpaz M: The molecular genetics of Philadelphia chromosome-positive leukemias. N Engl J Med 319:990, 1988

5. Ben-Neriah Z, Daley GQ, Mes-Masson AM, Witte ON, Baltimore D: The chronic myelogenous leukemia-specific P210 protein is the product of the *bcr-abl* hybrid gene. Science 233:212, 1986

6. Groffen J, Stephenson JR, Heisterkamp N, de Klein A, Bartram CR, Grosveld G: Philadelphia chromosomal breakpoints are clustered within a limited region, *bcr*, on chromosome 22. Cell 36:93, 1984

7. Gishizky ML, Witte ON: Initiation of deregulated growth of multipotent progenitor cells by *bcr-abl in vitro*. Science 256:836, 1992

8. Daley GQ, VanEtten RA, Baltimore D: Induction of chronic myelogenous leukemia in mice by the P210 *bcr-abl* gene of the Philadelphia chromosome. Science 247:824, 1990

9. Bedi A, Barber JP, Bedi GC, El-Deiry WS, Sidronsky D, Vala MS, Akhtar AJ, Hilton J, Jones RJ: *BCR-ABL*-mediated inhibition of apoptosis with delay of G_2/M transition after DNA damage: A mechanism of resistance to multiple anticancer agents. Blood 86:1148, 1995

10. Heisterkamp N, Groffen J: Molecular insight into the Philadelphia translocation. Hematol Pathol 5:1, 1991

11. Preston DL, Kusumi S, Tomonaga M, Izumi S, Ron E, Kuramoto A, Kamada N, Dohy H, Matsui T, Nonaka H, Thompson DE, Soda M, Mabuchi K: Cancer incidence in atomic bomb survivors. Part III: Leukemia, lymphoma and multiple myeloma, 1950-1987. Radiat Res 137:S68, 1994

12. Ito T: Induction of *BCR-ABL* fusion genes by *in vitro* X-irradiation. Jpn J Cancer Res 84:105, 1995

13. Nelson WG, Pienta KJ, Barrack ER, Coffey DS: The role of nuclear matrix in the organization and function of DNA. Annu Rev Biophys Chem 15:457, 1986

14. Laemmli UK, Kas E, Poljak L, Adachi Y: Scaffold-associated

regions: cis-acting determinants of chromatin structural loops and functional domains. Curr Opin Genet Dev 2:275, 1992

15. Garrard WT: Chromosomal loop organization in eucaryotic genomes, in Eckstein F, Lilley DM (eds): Nucleic Acids Molecular Biology. Heidelberg, Germany, Springer-Verlag, 1990, p 163

16. Lichter P, Cremer T, Borden J, Manuelidis L, Ward DC: Delineation of individual human chromosomes in metaphase and interphase cells by *in situ* hybridization using recombinant DNA libraries. Hum Genet 80:304, 1988

17. Manuelidis L: A view of interphase chromosomes. Science 250:1533, 1990

18. Haaf T, Schmid M: Chromosome topology in mammalian interphase nuclei. Exp Cell Res 192:325, 1990

19. Hochstrasser M, Sedat JW: Three-dimensional organization of *Drosophila melanogaster* interphase nuclei. II. Chromosome spatial organization and regulation. J Cell Biol 104:1471, 1987

20. Fox MH, Arndt-Jovin DJ, Jovin TM, Baumann PH, Robert-Nicaud M: Spatial and temporal distribution of DNA replication sites localized by immunofluorescence and confocal microscopy in mouse fibroblasts. J Cell Sci 99:247, 1991

21. Höfers C, Baumann P, Hummer G, Jovin TM, Arndt-Jovin DJ: The localization of chromosome domains in human interphase nuclei. Three-dimensional distance determinations of fluorescence *in situ* hybridization signals from confocal laser scanning microscopy. Bioimaging 1:96, 1993

22. Popp S, Scholl HP, Loos P, Jauch A, Stelzer E, Cremer C, Cremer T: Distribution of chromosome l8 and X centric heterochromatin in the interphase nucleus of cultured human cells. Exp Cell Res 189:1, 1990

23. De Boni V, Mintz AH: Curvilinear, three-dimensional motion of chromatin domains and nucleoli in neuronal interphase nuclei. Science 14:863, 1986

24. Bartholdi MF: Nuclear distribution of centromeres during the cell cycle of human diploid fibroblasts. J Cell Sci 99:255, 1991

25. Höfers C, Jovin TM, Hummer G, Arndt-Jovin DJ: The localization of chromosome domains in human interphase nuclei. Semi-automated two-dimensional image acquisition and analysis of fluorescence *in situ* hybridization signals. Bioimaging 1:107, 1993

26. Taniwaki M, Nishida K, Ueda Y, Misawa S, Nagai M, Tagawa S, Yamagami T, Sugiyama H, Abe M, Fukuhura S, Kashima K: Interphase and metaphase detection of the breakpoint of 14q32 translocations in B cell malignancies by double-color fluorescence in situ hybridization. Blood 85:3223, 1995

27. Height SE, Swansbury GJ, Matutes E, Treleaven JG, Catovsky D, Dyer MJS: Analysis of clonal rearrangements of the Ig heavy chain locus in acute leukemia. Blood 87:5242, 1996

28. Davi F, Gocke F, Smith S, Sklar J: Lymphocytic progenitor cell origin and clonal evolution of human B-lineage acute lymphoblastic leukemia. Blood 88:609, 1996

29. Strachman T, Read AP: Somatic mutations and cancer, in Human Molecular Genetics. Oxford, UK, BIOS Scientific, 1996, p 457

30. Dernburg AF, Broman KW, Fung JC, Marshall WF, Philips J, Agard DA, Sedat JW: Perturbation of nuclear architecture by long-distance chromosome interactions. Cell 85:745, 1996

31. Weimer R, Haaf T, Kruger J, Poot M, Schmid M: Characterization of centromere arrangements and test for random distribution in G_0, G_1, S, G_2, G_1 and early S phase in human lymphocytes. Hum Genet 88:673, 1992

32. Lichter P, Cremer T: Chromosome analysis by non-isotopic *in situ* hybridization, in Rooney DE, Czepulkowski BH (eds): Human Cytogenetics—A Practical Approach, Vol I. Oxford, UK, IRL, 1992, p 157

33. Kozubek M: Analysis of images obtained by fluorescence *in situ* hybridization. MSc thesis. Brno, Czech Republic, Masaryk University, 1995

34. Serra J: Image Analysis and Mathematical Morphology, Vol I. London, UK, Academic, 1994

35. Lukášová E, Kozubek S, Kozubek M, Kjeronská J, Rýznar L, Horáková J, Krahulcová E, Horneck G: Localization and distance between *ABL* and *BCR* genes in interphase nuclei of bone marrow cells of control donors and patients with chronic myeloid leukemia. Hum Genet (in press)

36. Natarajan AT: Mechanisms for induction of mutations and chromosome alterations. Environ Health Persp Suppl 101:225, 1993

37. Goodhead DT: Radiation tracks in biological materials: Initial damage in cells, DNA and associated structures, in Mendelson ML (ed): Genes, Cancer and Radiation Protection. Bethesda, MD, National Council on Radiation Protection and Measurements, 1992, p 25

38. Van Zeeland AA: DNA repair, in Obe G (ed): Mutations in Man. Berlin, Germany, Springer-Verlag, 1980, p 35

39. Goodhead DT, Thacker J, Cox R: Effects of radiations of different qualities on cells: Molecular mechanisms of damage and repair. Int J Radiat Biol 63:543, 1993

40. Simpson PJ, Savage JRK: Estimating the true frequency of X-ray-induced complex chromosome exchanges using fluorescence *in situ* hybridization. Int J Radiat Biol 67:37, 1995

41. Malyapa RS, Wright WD, Roti JLR: Radiation sensitivity correlates with changes in DNA supercoiling and nucleoid protein content in cells of three Chinese hamster cell lines. Radiat Res 140:312, 1994

42. Woudstra EC, Roesink JM, Rosemann M, Brunsting JF, Driessen C, Orta R, Konings AWT, Peacock JH, Kampinga HH: Chromatin structure and cellular radiosensitivity: A comparison of two human tumour cell lines. Int J Radiat Biol 70:693, 1996

1997 89: 4537-4545

Distribution of *ABL* and *BCR* Genes in Cell Nuclei of Normal and Irradiated Lymphocytes

S. Kozubek, E. Lukásová, L. Rýznar, M. Kozubek, A. Lisková, R.D. Govorun, E.A. Krasavin and G. Horneck

Blood (print ISSN 0006-4971, online ISSN 1528-0020), is published weekly by the American Society of Hematology, 2021 L St, NW, Suite 900, Washington DC 20036.